JOURNAL OF GEOPHYSICAL RESEARCH, VOL. 101, NO. A12, PAGES 27,555–27,564, DECEMBER 1, 1996

Ulysses observations of whistler waves at interplanetary shocks and in the solar wind

D. Lengyel-Frey,[1,2] R. A. Hess,[3] R. J. MacDowall,[4] R. G. Stone,[4] N. Lin,[5]
A. Balogh,[6] and R. Forsyth[6]

Abstract. This study of whistler wave emission observed by the Ulysses Unified Radio and Plasma Wave (URAP) experiment between 1 and 5 AU is a complement to previous studies of whistler waves observed by the Helios spacecraft between 0.3 and 1 AU. The Helios spacecraft continuously detected a background of whistlers close to the Sun, and this background was found to decrease in intensity with larger heliocentric distance. Ulysses plasma wave observations confirm this trend. Within a heliocentric distance of approximately 2 AU, whistler waves are routinely observed. Beyond about 3 AU the waves are usually observed only downstream of interplanetary shocks. Moreover, whistler waves are routinely observed within about 2 AU at all heliographic latitudes of the Ulysses trajectory (−80° to +80°). The combined observations from the Helios and Ulysses spacecraft suggest that whistler emission is always present in the solar wind, although at larger heliocentric distances the wave amplitudes are often below the thresholds of the URAP instrument. Observations throughout the first 5 years of the Ulysses mission show a clear correlation of whistler emission intensity with magnetic field strength, or gyrofrequency, such that increases in wave intensities coincide with increases in gyrofrequency. This correlation is especially evident in observations of interplanetary shocks and high-speed streams. A possible cause of this correlation is increased whistler wave growth due to enhanced electron temperature anisotropies in regions of compressed magnetic field. A shift of the background whistler spectrum as a function of gyrofrequency could account for the observed decrease in whistler amplitudes with increasing heliocentric distance.

1. Introduction

Studies have shown that magnetic wave activity at frequencies between the ion and electron cyclotron frequencies is prevalent in the solar wind. A ubiquitous background of waves continuously present in the solar wind was detected by the Helios spacecraft [*Neubauer et al.*, 1977a, b; *Beinroth and Neubauer*, 1981; *Denskat et al.*, 1983] between 0.3 and 1 AU. This background was found to increase by more than an order of magnitude over this distance range as the spacecraft approached the Sun. It was also found that the maximum observed wave frequency decreased with increasing heliocentric distance. The waves were observed up to a frequency of 470 Hz near 0.5 AU, but near 1 AU the maximum observed frequency was about 220 Hz. This whistler wave background was enhanced by the passage of interplanetary shocks and high-speed streams. Discrete bursts or wave enhancements of minutes or less, called "events," were also found, usually associated with magnetic structures such as directional and rotational discontinuities and magnetic holes. Further analyses of wave enhancements at interplanetary shocks and high-speed streams at 1 AU have been reported by *Gurnett et al.* [1979], *Kennel et al.* [1982], and *Coroniti et al.* [1982]. Preliminary studies of whistler waves observed at interplanetary shocks by the Ulysses spacecraft beyond 1 AU have been published [*Lengyel-Frey et al.*, 1992, 1994]. Observed magnetic to electric field amplitude ratios are similar to the computed index of refraction for whistler waves propagating parallel to the ambient magnetic field [*Gurnett et al.*, 1979; *Rodriguez and Gurnett*, 1975; *Coroniti et al.*, 1982], or at oblique angles [*Lengyel-Frey et al.*, 1994], which is consistent with the whistler interpretation of these waves.

In this paper we report Ulysses plasma wave observations of whistler waves at interplanetary shocks as well as in the solar wind with no shock association. We determine how whistler activity changes with heliocentric distance and latitude. We also discuss how Ulysses observations compare with Helios studies of whistler waves within 1 AU and offer an interpretation for the changes seen in whistler emission at interplanetary shocks and in the large-scale solar wind.

[1] Department of Astronomy, University of Maryland, College Park.
[2] Now at Johns Hopkins School of Medicine, Baltimore, Maryland.
[3] Hughes STX Corporation, Lanham, Maryland.
[4] NASA, Goddard Space Flight Center, Greenbelt, Maryland.
[5] School of Physics and Astronomy, University of Minnesota, Minneapolis, Minnesota.
[6] The Blackett Laboratory, Imperial College, London, England.

Paper number 96JA00548.
0148-0227/96/96JA-00548$09.00

2. Experiment Description

The Unified Radio and Plasma Wave (URAP) experiment [*Stone et al.*, 1992] on board the Ulysses spacecraft consists of five instruments for studying plasma wave phenomena over a frequency range of approximately 0.1 Hz to 1 MHz. The instrument relevant to this study is the wave form analyzer (WFA). An on-board spectral analysis of signals from both electric and magnetic field preamplifiers yields spectral data for 24 frequencies from approximately 0.1 to 500 Hz. Both peak and average amplitudes are returned with a time resolution of 64 s. We use the 64-s average WFA data as the basis of this study.

Data from the fluxgate magnetometer on Ulysses [*Balogh et al.*, 1992] is also used in this analysis. This instrument measures DC magnetic fields, and for this analysis we use 1-min field averages. In our study we also rely on identifications of shocks determined from the Ulysses magnetometer and plasma experiments [*Burton et al.*, 1992; *Balogh et al.*, 1994]. As of now, 154 shocks have been identified in Ulysses data. These shocks were observed from Ulysses launch in October 1990 to the early part of 1994, when the spacecraft attained a heliographic latitude of $-55°$.

3. Observational Analysis of Whistler Waves

3.1. Whistler Waves at Interplanetary Shocks

Significant low-frequency (0.2 to > 100 Hz) electromagnetic wave activity is routinely observed by the URAP WFA experiment in the solar wind when the spacecraft is within approximately 2 AU. These whistler waves are enhanced within high-speed streams. In addition, most interplanetary shocks identified by Ulysses are associated with these waves. The waves are enhanced in the compressed, downstream regions of the shocks. For shocks beyond approximately 3 AU, upstream emission is rarely observed.

Figure 1a shows 64-s average magnetic wave amplitude $\tilde{B}$ observed at 9 Hz 8 hours before and after passage of the April 7, 1991 forward shock at Ulysses. The spacecraft was at 2.6 AU at this time. Shock passage is marked in Figure 1a by the vertical dashed line. This is accompanied by a sudden enhancement in wave activity, which persists for many hours after shock passage in the downstream region, that is, the region of plasma compressed by the shock. The noise upstream of the shock is mainly instrumental background noise. The downstream wave activity is highly variable, but there is a gradual decrease after shock passage, reflecting the eventual return of the plasma to preshock conditions. All interplanetary shocks show whistler wave enhancements in the downstream region. Typical durations of observed downstream activity at shocks are 12 to 18 hours. In Figure 1b we plot the corresponding magnetic field strength observed for the April 7 shock. As for the wave observations, the magnetic field shows an abrupt increase in strength at shock passage, and this field enhancement persists far into the downstream region.

It is instructive to plot whistler activity observed for all Ulysses shocks. In Figure 2a we plot magnetic wave amplitude at 5 Hz observed for 8 hours downstream of each Ulysses shock, where each symbol represents an average of 1 hour of data. The horizontal axis is time of shock measured in fractional year (91.0 is January 1, 1991). There is a decrease in wave amplitude throughout the early mission until about 1992, after which emission levels are close to instrumental background (about 0.0015 $\gamma/\sqrt{\text{Hz}}$). In Figure 2b we plot the measured electron gyrofrequency f_{ce}, which is proportional to magnetic field strength. There is again an obvious correlation between field strength, measured by the gyrofrequency, and whistler activity. The gyrofrequency shows behavior similar to the wave behavior, namely, the field decreases through the early part of the mission and becomes relatively constant beginning in early 1992. The high-latitude phase of the mission began during the early part of 1992 when the spacecraft attained a southern latitude of $-10°$. The last shock plotted was observed at a latitude of $-55°$. We see that downstream whistler waves are observed throughout the range of latitude of this shock sample.

It is also instructive to make plots similar to Figure 2 but for upstream observations. These plots are shown in Figures 3a and 3b, where 8 hours of upstream data are plotted for each

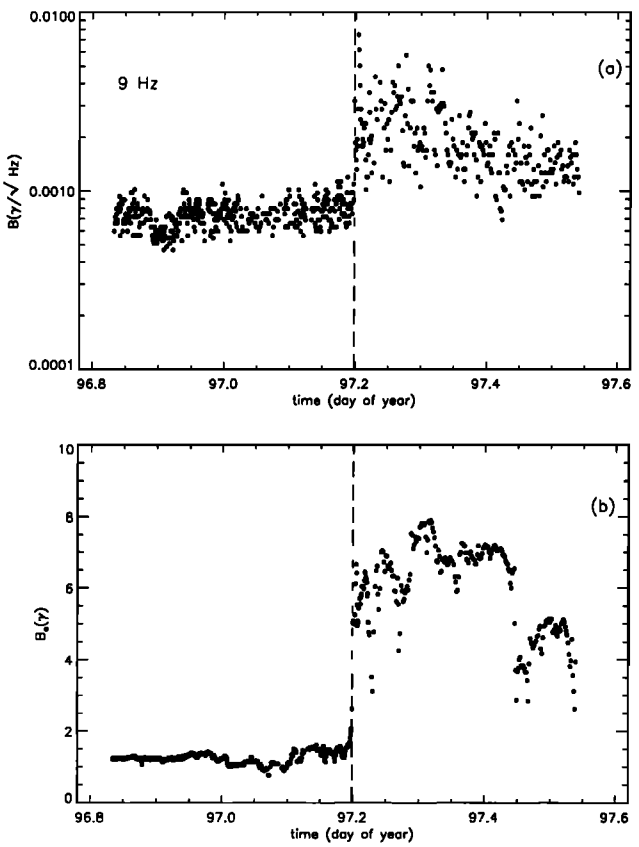

Figure 1. (a) Magnetic wave amplitude at 9 Hz versus time in day of year for 17-hour interval centered on the April 7, 1991 shock. Time of shock passage at 0446 UT is marked by vertical dashed line. (b) Magnetic field strength is shown for same interval.

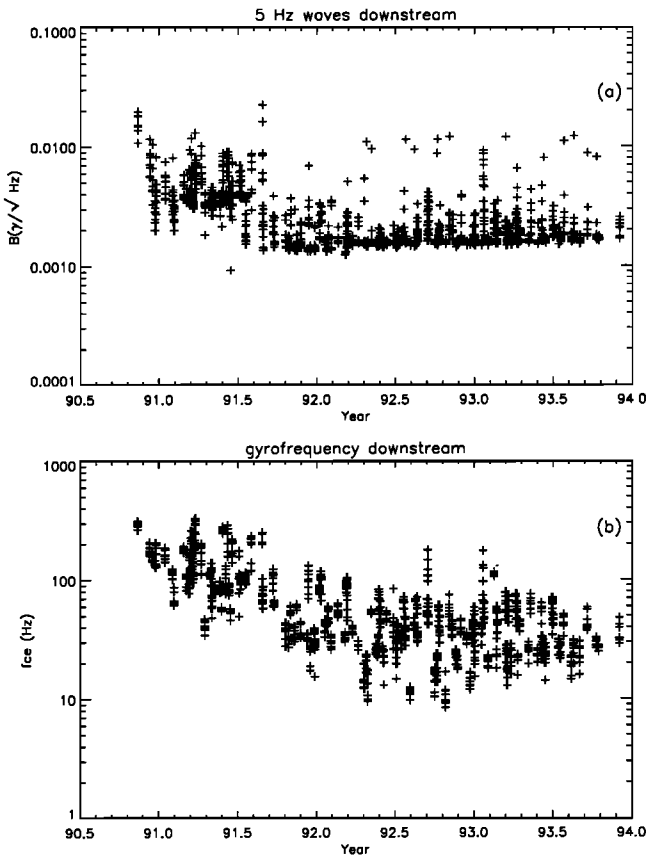

Figure 2. (a) Magnetic wave amplitude at 5 Hz versus time in fractional year. Data for 8 hours downstream of each shock is shown, with each symbol representing a 1-hour average. The background level is at about 0.0015γ. (b) Electron gyrofrequency versus time in fractional year. Data points are 1-hour averages downstream and correspond to points in Figure 2a. Similar trends are seen in both plots.

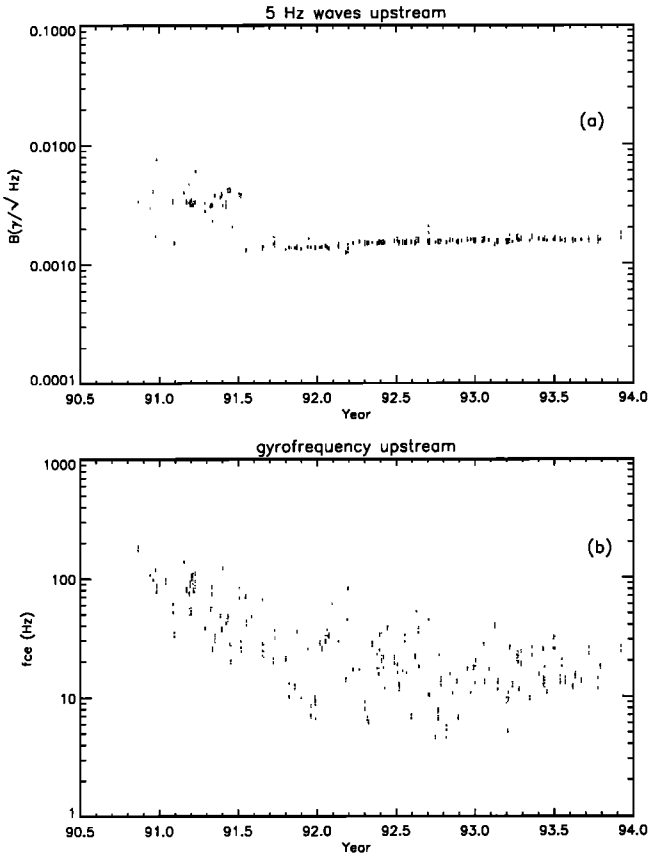

Figure 3. (a) Same as for Figure 2a but for waves observed within 8 hours upstream of each shock. (b) Same as for Figure 2b but for gyrofrequencies observed upstream of shocks. At this frequency, waves are generally not observed when the gyrofrequency is less than about 40 Hz.

shock, and each point represents a 1-hour average. Again, we note the decrease in upstream wave amplitudes and f_{ce} with time for the early part of the mission. However, after about the middle of 1991 there is typically only instrumental noise observed upstream of shocks. The disappearance of upstream wave activity coincides with a decrease in f_{ce} to below 40 Hz. This suggests that for 5-Hz whistler waves to be observed above the WFA instrumental threshold, the corresponding gyrofrequency must exceed 40 Hz. Thresholds for wave observations at other frequencies are also related to gyrofrequency. For example, for 9-Hz observations f_{ce} generally must exceed about 80 Hz for whistlers to be observable.

The correlation between whistler wave amplitude and local magnetic field strength is demonstrated more directly in Figure 4, in which we plot 5-Hz wave amplitudes versus gyrofrequency for about 75 in-ecliptic shocks observed early in the Ulysses mission. The data are 1-hour averages downstream of each shock. This shock sample is chosen since the wave amplitudes associated with these shocks have levels well above the instrumental threshold, which is at about $0.0015\ \gamma/\sqrt{\text{Hz}}$ at this frequency. The linear correlation coefficient of the data is 0.67. We note that the correlation is clear only over a significant range of f_{ce}; that is, for observations with f_{ce} values ranging over a factor less than about 2, the correlation is less obvious owing to the inherent burstiness of the emission. Possible reasons for the correlation are considered in section 4.

A previous study reported no correlation between observed wave amplitudes and measured shock properties, such as Mach number or shock normal angle θ_{Bn} [*Lengyel-Frey et al.*, 1992], although this study was based on a small sample of about 20 Ulysses shocks. We have since confirmed this conclusion for the larger sample of 75 in-ecliptic shocks, discussed above. Figure 5a is a plot of 5-Hz wave amplitudes observed downstream of the shocks versus shock normal angle, using hour averages of the wave data. A linear least squares fit to the data is shown by the solid line. Although a slight trend of increasing amplitude for more perpendicular shocks (larger θ_{Bn}) is evident, this seems to be associated with the slight increase in downstream magnetic field strength with increasing θ_{Bn}, shown in Figure 5b. Similar results have been found with the highest resolution data (64 sec) for intervals of less than 15 min from shock passage. Consequently, we find no evidence that shock normal angle

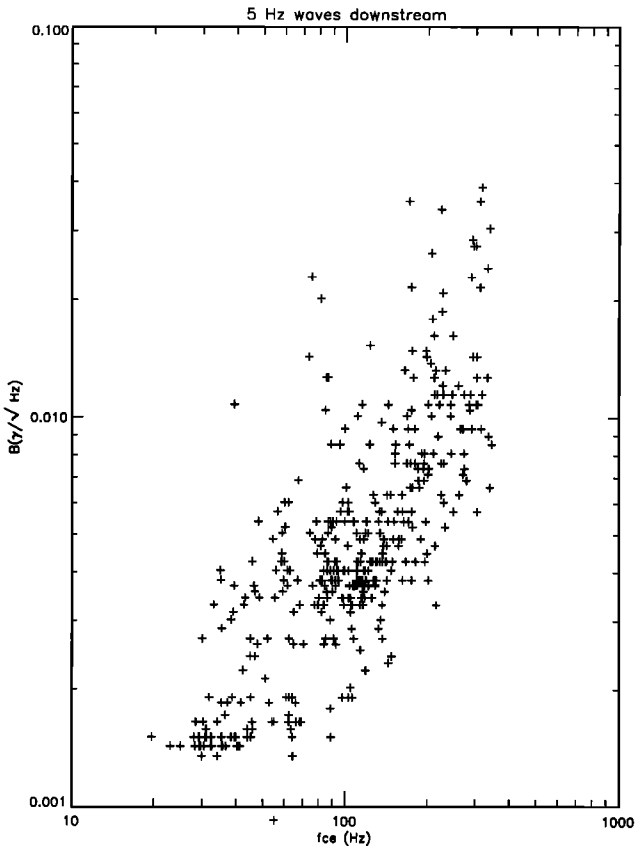

Figure 4. Magnetic wave amplitude at an observing frequency of 5 Hz versus gyrofrequency for in-ecliptic shocks. Each point represents 1-hour average data observed downstream of a shock. A clear correlation of wave amplitude and gyrofrequency is evident.

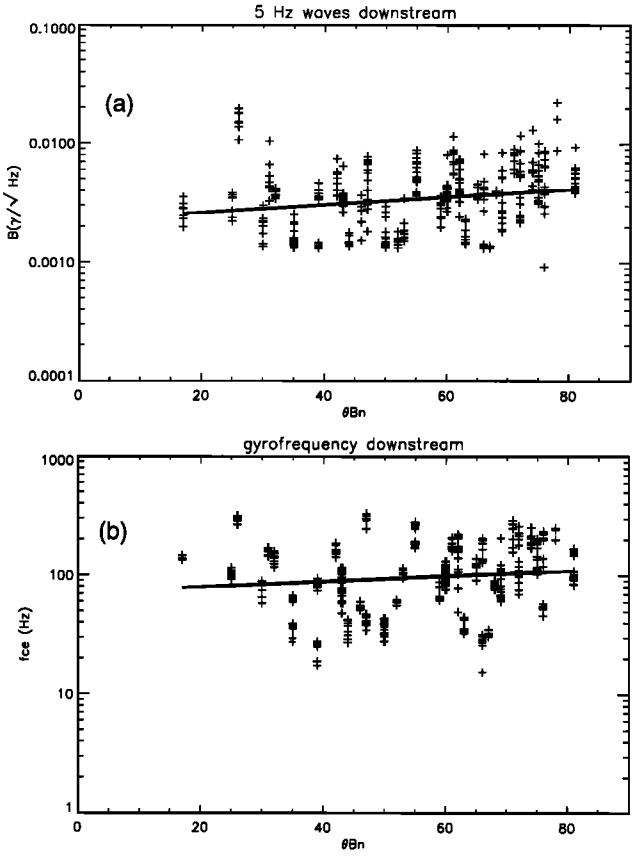

Figure 5. (a) Wave amplitude at 5 Hz versus shock normal angle using 1-hour average data downstream of 75 in-ecliptic shocks. A least squares fit to the data is shown by the solid line. (b) Gyrofrequency versus shock normal angle, corresponding to points in Figure 5a. Although there appears to be a weak correlation between amplitude and θ_{Bn}, this is just due to the slight correlation of f_{ce} and θ_{Bn}.

plays a role in whistler wave activity at interplanetary shocks.

We note that in a study of Earth's bow shock, whistlers from the bow shock transition region (observed within minutes of shock passage) were found to be of greater amplitude for more perpendicular shocks [*Rodriguez and Gurnett,* 1975]. We suggest that the apparent discrepancy between our results and bow shock studies could be explained if waves observed at interplanetary shocks are generated far from the shock transition region, whereas bow shock related waves are produced in the shock front; bow shock whistlers would then be affected by conditions intrinsic to the shock front, such as θ_{Bn}. The relatively low time resolution of WFA data would make it difficult to isolate those waves produced from the rapidly passing shock transition region from waves generated in the shock wake.

3.2. Whistler Waves in the Solar Wind

Whistler waves are routinely observed for extended periods in the solar wind within heliocentric distances of approximately 2 AU. We will refer to such occurrences simply as whistler activity in the solar wind. Figure 6a shows a prolonged interval of wave activity at 5 Hz during November 1990 when Ulysses was within 1.2 AU. The time axis is in day of year. This interval is characterized by gradual increases and decreases in average wave amplitudes, with minimum observed levels at the instrumental background (about 0.0015 $\gamma/\sqrt{\text{Hz}}$ at 5 Hz). Slowly varying whistler emission observed by the Helios spacecraft has been referred to as the whistler background, upon which is superposed short duration (minutes or less) activity called events [*Neubauer et al.,* 1977a, b]. Both background and short bursts are evident in Figure 6a. In Figure 6b we plot the associated gyrofrequency for the same interval. For this interval there is only one shock observed, and this is on day 315 at 2035 UT. Most of the wave activity present during this interval is related to high-speed streams rather than shocks.

The wave activity is clearly correlated with the magnetic field strength, with higher wave amplitudes occurring when the field strength increases. However, the wave activity is very bursty, and for a given field strength there is a range in amplitudes of individual bursts. Along with a correlation of average wave amplitude with field strength, there appears to be a correlation of wave burstiness with the amount of variation in the field magnitude. For days 326 to 330 the wave activity is relatively constant in amplitude. For this interval the gyrofrequency is about 100 Hz and varies little. In contrast,

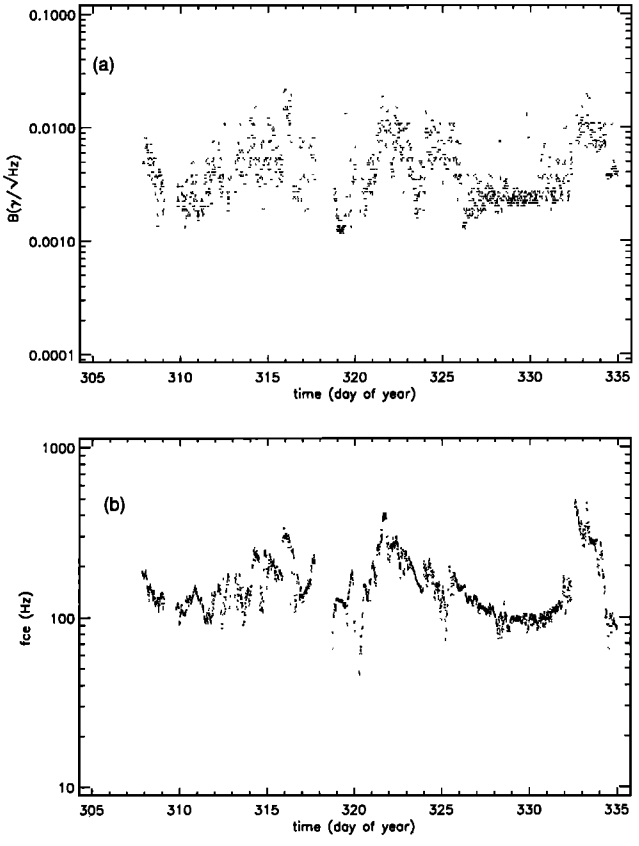

Figure 6. (a) Magnetic wave amplitude at 5 Hz versus time in day of year, for November 1990. For this frequency instrumental threshold is about 0.0015 $\gamma/\sqrt{\text{Hz}}$. The whistler emission is very bursty, but there are gradual increases and decreases in the background over many days. (b) Gyrofrequency from Ulysses magnetometer observations for same time period. There is a general correlation between gyrofrequency and wave amplitudes. Only one interplanetary shock was observed during this period on day 315 at 2035 UT. Major field enhancements are related to high-speed streams. The period of the least magnetic field variability (days 326 to 332) is associated with the least wave activity.

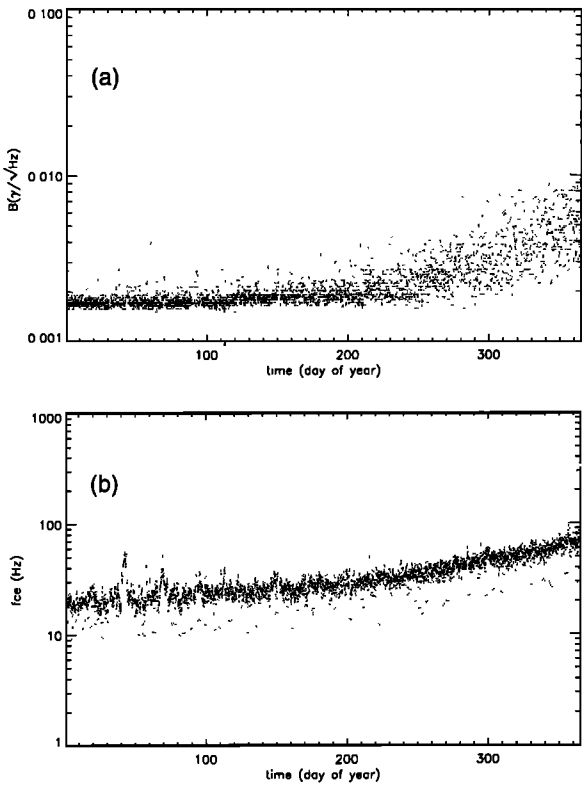

Figure 7. (a) Whistler wave amplitudes at 5 Hz during 1994. Time axis is day of year. Interval spans heliocentric distance 3.8 AU at start of interval to 1.5 AU at end of interval. Latitude range is −48° at start of interval, −80° near day 200, and −44° at end of plotted data. Until day 200 at about 2.6 AU, little activity above instrumental threshold is seen. (b) Corresponding gyrofrequency is shown. Gradual increase in wave activity after about day 200 parallels the rise in gyrofrequency beyond 40 Hz.

the other intervals shown in the plot display large variations in both wave amplitude and magnetic field strength. It therefore appears that whistler wave activity is related to magnetic field strength, as well as to magnetic field variation.

During most of the Ulysses mission the spacecraft has been beyond 3 AU, and for most of the mission, whistler activity has not been observed in the solar wind. During 1994 the spacecraft traversed the range from approximately 4 AU to 1.5 AU. A plot of whistler activity at 5 Hz is shown for 1994 in Figure 7a. The horizontal axis is day of year during 1994. Corresponding gyrofrequencies are shown in Figure 7b. At the start of this interval the spacecraft was at a heliographic latitude of −48°. It reached its most southern latitude of −80° in September 1994 (about day 200). It then proceeded northward, reaching −44° at the end of the interval. During this interval the spacecraft steadily decreased in heliocentric distance from 3.8 to 1.5 AU. Figure 7a shows that before day 200, when the spacecraft is at about 2.6 AU, only sporadic wave activity is observed. Some of this activity is associated with interplanetary shocks. After this time, as Ulysses approaches closer to the Sun, the whistler activity gradually increases and becomes almost continuously observable in the solar wind. The gyrofrequency shows a steady increase with decreasing heliocentric distance. The wave activity becomes almost continuously present when the gyrofrequency becomes 40 Hz or greater. Note that the wave activity does not show a dependence on latitude. The steady increase in emission after day 200 corresponds to the increase in gyrofrequency associated with the decrease in heliocentric distance.

Figure 8 shows the interval between August 1994 and August 1995. This interval covers the range from −80° to +80° of Ulysses latitude. The spacecraft passed through the ecliptic plane at about 95.2 (March, 1995). At the start of the interval, Ulysses was at 2.4 AU and reached its smallest heliocentric distance 1.3 AU near 95.2. It then moved outward and reached 2 AU at the end of the interval. Figure 8a shows 5-Hz wave amplitudes which increase with decreasing heliocentric distance. Within about 20° of the ecliptic plane the waves become heavily modulated in association with ex-

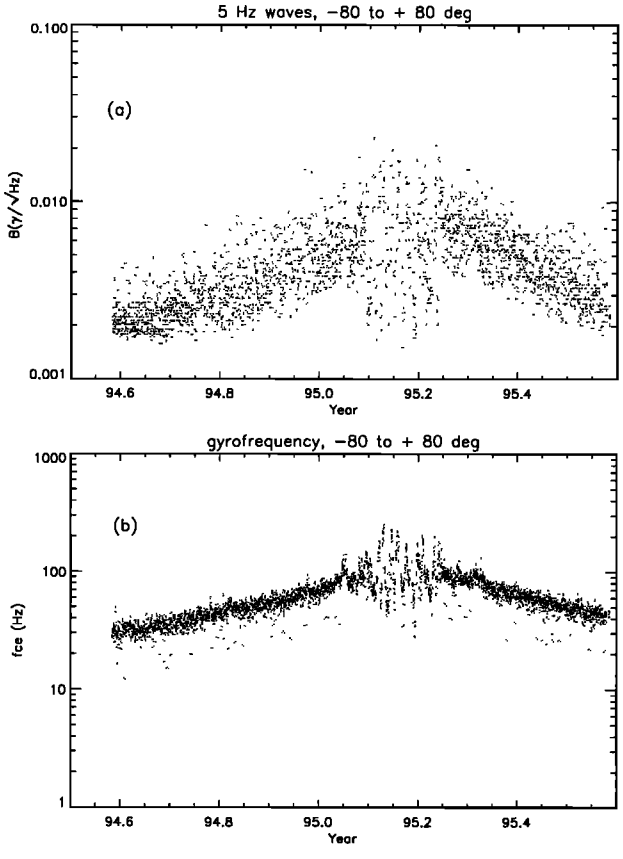

Figure 8. Plots similar to Figure 7 but for interval from August 1994 to August 1995. Heliocentric distances vary from 2.4 AU at beginning, to 1.3 AU near 95.2, to 2 AU at the end. This interval spans −80° at the start, to 0° near 95.2, to +80° at the end. The variation in wave amplitude closely follows the variation in gyrofrequency. Within 20° of the ecliptic plane (95.0 to 95.3) modulation due to repeated passage through the streamer belt is evident.

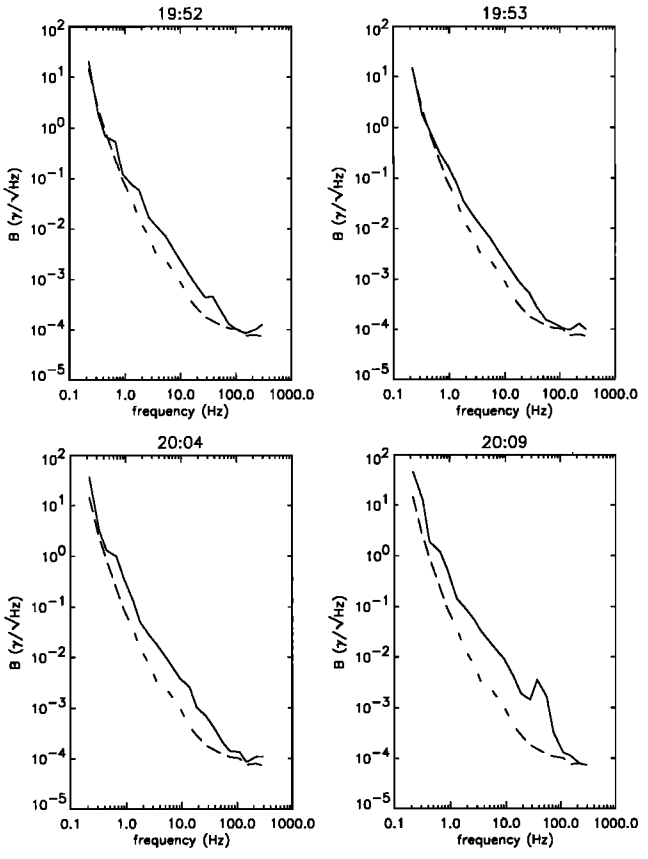

Figure 9. Several examples of spectra (solid lines) of whistler bursts downstream of the December 9, 1990 shock. The spectra are decreasing power laws with spectral indices of about −1.8, similar to spectra observed in the solar wind both by Ulysses and Helios spacecraft. Dotted lines mark the instrumental threshold.

cursions through corotating high-speed streams. Figure 8b shows the gyrofrequency for this interval. The gradual rise in gyrofrequency throughout this period, as well as the rapid variations which coincide with the wave modulation are evident. We would conclude from this plot that whistler wave activity throughout the heliographic latitude range is primarily determined by gyrofrequency, in the same manner as for waves in the ecliptic. Figures 7 and 8 demonstrate that latitude by itself is not a determining factor in the occurrence of whistler wave activity.

3.3. Whistler Wave Spectra

Figure 9 shows some typical whistler spectra, plots of wave amplitude versus frequency, observed downstream of the shock of December 9, 1990. The spectra are generally monotonically decreasing functions of frequency with no significant emission at frequencies above the local gyrofrequency (about 200 Hz for the plots shown). Although most whistler spectra are relatively featureless, there are exceptions, as shown, for example, in the spectrum from 20:09 UT. From least squares fits of spectral data to a power law function $\tilde{B} \propto f^{-\alpha}$ we find the spectral index α to be 1.8 ± 0.1 for whistler waves associated with interplanetary shocks. An analysis of the spectra of waves in the solar wind gives similar results, namely, $\alpha \approx 1.7 \pm 0.1$. These results agree well with spectral indices determined by the Helios spacecraft for whistlers in the solar wind from 0.3 to 1 AU [*Neubauer et al.*, 1977b], suggesting that whistlers associated with interplanetary shocks have the same basic properties as those produced in the large scale solar wind.

The well-known whistler wave dispersion relation [*Stix*, 1962] restricts these waves to frequencies below the local electron gyrofrequency. To demonstrate the dependence of wave frequency on the gyrofrequency, we replot wave spectra in terms of the ratio of observing frequency f to the local gyrofrequency f_{ce}, as shown in Figure 10. The data shown in this plot are 1-hour averages occurring within 8 hours downstream of 75 in-ecliptic shocks. All wave amplitudes above instrumental thresholds are plotted. In each case the wave frequency f is divided by the observed local gyrofrequency to yield a value of f/f_{ce}. The observed waves have frequencies which fall approximately between the ion gyrofrequency ($f/f_{ce} \approx .001$) and the electron gy-

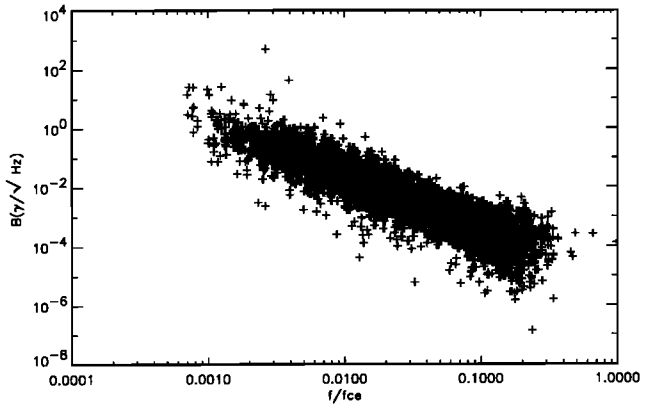

Figure 10. Wave amplitude versus ratio of wave frequency to gyrofrequency for observations of waves above instrumental threshold. Each point represents 1-hour average data downstream of an in-ecliptic shock. The observations cover the spectral range $\approx$ 0.2 Hz to 300 Hz. Typical values of f/f_{ce} are between 0.01 and 0.1.

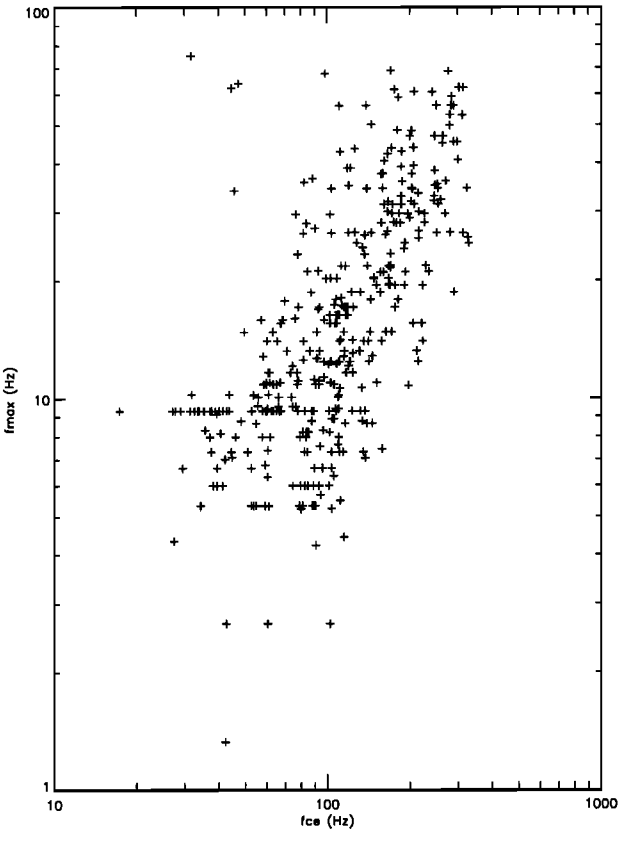

Figure 11. Maximum frequency of observed spectrum versus gyrofrequency for in-ecliptic shocks. Each cross is maximum frequency during a 1-hour interval downstream of a shock. Maximum frequency increases with f_{ce} suggesting that whistler spectra shift in frequency range as a function of gyrofrequency.

rofrequency ($f/f_{ce} = 1$). The absence of waves above f_{ce} is consistent with the whistler dispersion relation. Few waves are observed near the ion gyrofrequency, in part because instrumental backgrounds increase with decreasing frequency, making it difficult to observe waves at the lowest frequencies. We find typical values of f/f_{ce} to be between approximately 0.01 and 0.1. There is a tight correlation of amplitude $\tilde{B}$ and f/f_{ce}, although for a given f/f_{ce} value there is a wide range in observed wave amplitudes. The bulk of observations occur at frequencies well below the electron gyrofrequency. These results have implications for whistler instability mechanisms, as will be discussed in section 4.

We have determined the maximum observed wave frequency for whistler spectra, that is, the maximum frequency for which the waves are observed above instrumental background. Figure 11 shows a correlation between maximum wave frequency $f_{\max}$ and f_{ce}, with $f_{\max}$ increasing with increasing f_{ce}. This correlation demonstrates that the whistler spectrum undergoes shifts in frequency range and that these shifts correlate with changes in the local gyrofrequency. The whistler dispersion relation restricts wave frequencies to values below f_{ce}, and therefore a shift of the spectrum toward higher frequencies as f_{ce} increases would be expected. From this plot it is evident that $f_{\max}/f_{ce}$ is about 0.1, implying once again that f/f_{ce} is less than 0.1 in most cases.

4. Discussion

A number of instability mechanisms have been proposed for whistler waves (see *Schwartz* [1980] for a review). The most likely instabilities for typical solar wind conditions are the whistler anisotropy instability [*Kennel and Petschek,* 1966] and electron heat flux instability [*Gary and Feldman,* 1977]. In the former case the electrons have a bi-Maxwellian distribution, with $T_\perp/T_\parallel > 1/(1 - f/f_{ce})$, where $T_\perp$ is perpendicular electron temperature, $T_\parallel$ is parallel temperature, and $0 < f/f_{ce} < 1$. Therefore for wave growth to occur, it is necessary that $T_\perp/T_\parallel > 1$, and larger temperature ratios have been found to yield larger growth rates [*Gary and Madland,* 1985]. We note that this instability is more easily excited for smaller f/f_{ce} ratios and that the observed distribution of f/f_{ce} for whistlers shown in Figure 10 is between 0.01 and 0.1. This indicates that $T_\perp/T_\parallel$ need only be slightly greater than 1 for this instability to occur. In studies of electron distributions observed by Ulysses at several interplanetary shocks [*Solomon et al.,* 1995; *Pierre et al.,* 1995], values of $T_\perp/T_\parallel$ ranging from 1 to 3 were frequently determined from downstream observations. Such values imply whistler wave growth and suggest that temperature anisotropies are a source of whistler generation downstream of shocks.

The whistler heat flux instability occurs in a plasma characterized by two bi-Maxwellian distributions, a core and halo, and where a relative velocity drift between the components occurs along the magnetic field. These conditions are typical in the solar wind near 1 AU [*Feldman et al.,* 1975]. The instability is sensitive to temperature anisotropies of the halo component [*Gary et al.,* 1994], specifically $T_{h\perp}/T_{h\parallel} \leq 1$. This is a condition which *Scime et al.* [1995] have found in an interval during observed whistler activity. *Scime et al.* [1995] have also found that this activity is correlated with de-

creases in the solar wind heat flux. These observations suggest that heat flux instabilities might be a cause of at least some whistler wave activity in the solar wind.

The whistler background may also be due to a nonlinear cascade in which low-frequency Alfven waves merge to produce waves of higher frequency. Spectra below the ion gyrofrequency f_{ci} have a Kolmogorov-type power law slope ($-5/3$ for power spectra or about -1.3 for amplitude spectra). Steeper spectra at frequencies greater than f_{ci} are observed for whistler waves, such as shown in Figure 9 where power law spectral indices are typically about -1.8. The spectral steepening has been investigated by *Ghosh et al.* [1996], using magnetohydrodynamic equations including the Hall term. Their simulations show that for certain combinations of magnetic helicity and cross helicity the cascade of left circularly polarized (LCP) waves is suppressed at f_{ci}, whereas right circularly polarized (RCP) waves are not affected. This would account for a steepening of the spectrum above f_{ci}. The cascade through the proton gyrofrequency therefore allows the generation of RCP waves, such as whistlers, and might provide an explanation for the ubiquitous whistler background. The increase in Alfven wave energy in regions of greater magnetic compression might account for higher amplitude whistlers associated with larger magnetic field strengths, although this has not been simulated (S. Ghosh, private communication, 1995). The Ghosh et al. results are preliminary because a realistic simulation must also include wave-particle interactions at f_{ci}, which have not yet been taken into account. The results, however, do suggest the possibility that the whistler background is associated with a nonlinear cascade mechanism.

In the earlier Helios spacecraft studies of whistler waves [*Neubauer et al.*, 1977a, b] the authors suggested that the observed decrease in average whistler amplitude and magnetic field strength with radial distance was merely a coincidence and was not due to any direct dependence of wave amplitude on the magnetic field strength. It seems likely, however, that the wave amplitudes and field strengths are directly related. The correlation of whistler amplitude and gyrofrequency over a range of heliocentric distance, as well as at shocks in high-speed streams suggests a physical relationship between these phenomena. Magnetic field compression is associated with enhancements of $T_\perp$ relative to $T_\parallel$. Electrons heated within such compressions easily propagate along field lines, such that electrons with large $T_\parallel$ escape heated regions and remaining electrons have an excess of perpendicular energy [*Gary*, 1993]. This results in increased growth of whistlers owing to enhanced temperature anisotropies. Compressed regions downstream of shocks and in high-speed streams are likely sites of enhanced whistler activity. Whether this effect would account for larger whistler amplitudes at smaller heliocentric distances remains a question. It is clearly necessary to determine temperature anisotropy ratios over a large heliocentric distance range using Ulysses and Helios observations.

Another possible cause of the correlation between field strength and whistler amplitudes might be that a variation in gyrofrequency causes a frequency shift of the whistler background spectrum. This idea is illustrated in Figure 12. The whistler spectrum is a monotonically decreasing power law, and the spectrum is restricted to frequencies below the local electron gyrofrequency because of the whistler dispersion relation. The spectrum therefore may shift with f_{ce}, as illustrated in Figure 12. Wave amplitude at a given observing frequency will appear greater for larger f_{ce} owing to the spectral shift across the frequency range. Thus the decrease in whistler amplitudes with heliocentric distance may be a consequence of the the shift of the background whistler spectrum toward lower frequencies as f_{ce} decreases with increasing distance from the Sun. The increase in maximum whistler wave frequency as f_{ce} increases (shown in Figure 11) suggests that the whistler spectrum undergoes some displacement which is dependent on f_{ce}.

5. Summary and Conclusions

We have examined whistler wave properties observed at interplanetary shocks and in the solar wind by the Ulysses URAP wave experiment. The main conclusions of this study are as follows:

1. Ulysses observations of whistler waves between 1 and 5 AU confirm the trends found by earlier Helios observations between 0.3 and 1 AU. Both spacecraft routinely observe a background of whistler waves in the solar wind, and this background decreases in intensity with heliocentric distance. Beyond about 3 AU the waves are normally below URAP instrumental thresholds.

2. Whistler waves are observed downstream of almost all Ulysses shocks and are observed upstream when the spacecraft is within a heliocentric distance of about 2 AU. Whistler amplitude spectra at shocks and in the solar wind obey power

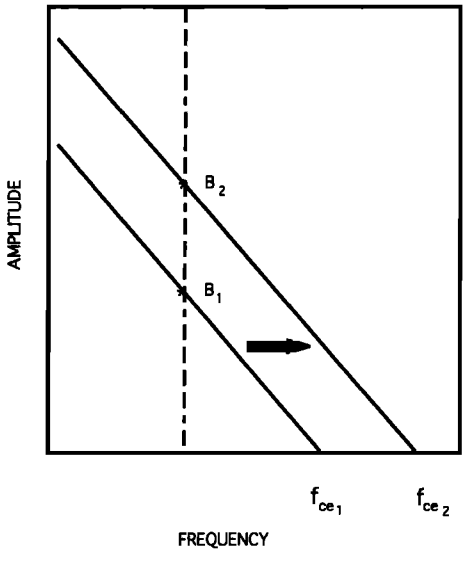

Figure 12. A schematic drawing of idealized whistler spectra which shift in frequency range depending on the associated gyrofrequency. This demonstrates that whistler wave amplitudes are likely to be enhanced when gyrofrequency is greater, owing to a spectral shift to the right.

laws with spectral indices of approximately -1.8 ± 0.1. This is consistent with Helios spacecraft results obtained in the solar wind between 0.3 and 1 AU. There is no obvious correlation of wave amplitude and shock normal angle θ_{Bn}. This suggests that whistlers associated with interplanetary shocks are not affected by properties of the shock front (probably because these waves are generated far from the shock transition region). The similarity of whistler properties upstream and downstream of shocks and in the ambient solar wind suggests that common mechanisms account for the whistler background in all of these regions.

3. Whistler activity is observed at all heliographic latitudes. The whistler background at high heliographic latitudes shows the same dependence on gyrofrequency as for whistlers in the ecliptic plane; that is, high-latitude background whistlers are observed when Ulysses is within approximately 2 AU, and the wave amplitudes decrease with increasing heliocentric distance. Whistler waves are strongly modulated when passing through the streamer belt near the ecliptic plane, as a consequence of the strong modulation of gyrofrequency in this region.

4. There is a clear correlation of wave amplitude with magnetic field strength, or electron gyrofrequency. As the gyrofrequency increases, average wave amplitudes are observed to increase. This correlation may be due, in part, to enhanced $T_\perp/T_\parallel$ electron temperature anisotropies in regions of magnetic field compression. Another possible cause of the correlation is a shifting of the whistler spectrum as local gyrofrequency varies. An increase in gyrofrequency would result in an increase in amplitude at a given frequency due to a shift of the monotonically decreasing spectrum toward higher frequency. It is important to study electron distributions at interplanetary shocks, in high speed streams, and over a large range of heliocentric distance to understand changes in whistler activity observed in these regions.

5. Whistler wave frequencies are observed to be between the ion and electron gyrofrequencies. Most waves have maximum frequencies well below the local gyrofrequency. The observation that most wave frequencies are between 0.01 and 0.1 f_{ce} implies that $T_\perp/T_\parallel$ need not be much greater than 1 for wave growth to occur.

Acknowledgments. The URAP investigation is a collaboration of NASA/Goddard Space Flight Center, the Observatoire de Paris-Meudon, the University of Minnesota, and the Centre des Etudes Terrestres et Planetaires, Velizy, France.

The Editor thanks F. M. Neubauer and E. Scime for their assistance in evaluating this paper.

References

Balogh, A., T. J. Beek, R. J. Forsyth, P. C. Hedgecock, R. J. Marquedant, E. J. Smith, D. J. Southwood, and B. T. Tsurutani, The magnetic field investigation on the Ulysses mission: Instrumentation and preliminary science results, *Astron. Astrophys. Suppl. Ser., 92,* 221, 1992.

Balogh, A., J. A. Gonzalez-Esparaz, R. J. Forsyth, M. E. Burton, B. E. Goldstein, E. J. Smith, S. J. Bame, Interplanetary shock waves: Ulysses observations in and out of the ecliptic plane, *Space Sci. Rev., 72,* 171, 1994.

Beinroth, H. J., and F. M. Neubauer, Properties of whistler mode waves between 0.3 and 1.0 AU from Helios observations, *J. Geophys. Res., 86,* 7755, 1981.

Burton, M. E., E. J. Smith, B. E. Goldstein, A. Balogh, and S. J. Bame, Ulysses: Interplanetary shocks between 1 and 4 AU, *Geophys. Res. Lett., 19,* 1287, 1992.

Coroniti, F. V., C. F. Kennel, F. L. Scarf, and E. J. Smith, Whistler mode turbulence in the disturbed solar wind, *J. Geophys. Res., 87,* 6029, 1982.

Denskat, K. U., H. J. Beinroth, and F. M. Neubauer, Interplanetary magnetic field power spectra with frequencies from 2.4×10^{-5} Hz to 470 Hz from Helios: observations during solar minimum conditions, *J. Geophys., 54,* 60, 1983.

Feldman, W. C., J. R. Asbridge, S. J. Bame, M. D. Montgomery, and S. P. Gary, Solar wind electrons, *J. Geophys. Res., 80,* 4181, 1975.

Gary, S. P., E. E. Scime, J. L. Phillips, and W. C. Feldman, The whistler heat flux instability: Threshold conditions in the solar wind, *J. Geophys. Res., 99,* 23, 1994.

Gary, S. P., *Theory of Space Plasma Microinstabilities*, Cambridge Univ. Press, New York, 1993.

Gary, S. P., and W. C. Feldman, Solar wind heat flux regulation by the whistler instability, *J. Geophys. Res., 82,* 1087, 1977.

Gary, S. P., and C. D. Madland, Electromagnetic electron temperature anisotropy instabilities, *J. Geophys. Res., 90,* 7607, 1985.

Ghosh, S., E. Siregar, D. A. Roberts, and M. L. Goldstein, Simulation of high frequency solar wind power spectra using Hall magnetohydrodynamics, *J. Geophys. Res., 101,* 2493, 1996.

Gurnett, D. A., F. M. Neubauer, and R. Schwenn, Plasma wave turbulence associated with an interplanetary shock, *J. Geophys. Res., 84,* 541, 1979.

Kennel, C. F., and H. E. Petschek, Limit on stably trapped particle fluxes, *J. Geophys. Res., 71,* 1, 1966.

Kennel, C. F., F. L. Scarf, F. V. Coroniti, E. J. Smith, and D. A. Gurnett, Nonlocal plasma turbulence associated with interplanetary shocks, *J. Geophys. Res., 87,* 17, 1982.

Lengyel-Frey, D., R. J. MacDowall, R. G. Stone, S. Hoang, F. Pantellini, P. Canu, N. Cornilleau-Wehrlin, A. Balogh, and R. Forsyth, Plasma wave phenomena observed at interplanetary shocks by the Ulysses URAP experiment, in Proceedings of the 26th ESLAB Symposium - Study of the Solar-Terrestrial System, *Eur. Space Agency Spec. Publ., ESA SP-346,* 71, 1992.

Lengyel-Frey, D., W. M. Farrell, R. G. Stone, A. Balogh, and R. Forsyth, An analysis of whistler waves at interplanetary shocks, *J. Geophys. Res., 99,* 13,325, 1994.

Neubauer, F. M., H. J. Beinroth, H. Barnstorf, and G. Dehmel, Initial results from the Helios-1 Search Coil Magnetometer Experiment, *J. Geophys. Res., 42,* 599, 1977a.

Neubauer, F. M., G. Musmann, and G. Dehmel, Fast magnetic fluctuations in the solar wind: Helios 1, *J. Geophys. Res., 82,* 3201, 1977b.

Pierre, F., J. Solomon, N. Cornilleau-Wehrlin, P. Canu, E. E. Scime, and J. L. Phillips, Whistler-mode wave generation around interplanetary shocks in and out of the ecliptic plane, *Geophys. Res. Lett., 22,* 3425, 1995.

Rodriguez, P., and D. A. Gurnett, Electrostatic and electromagnetic turbulence associated with the Earth's bow shock, *J. Geophys. Res., 80,* 19, 1975.

Schwartz, S., Plasma instabilities in the solar wind: A theoretical review, *Rev. Geophys. Space Sci., 18,* 313, 1980.

Scime, E. E., S. J. Bame, W. C. Feldman, S. P. Gary, and J. L. Phillips, Regulation of the solar wind heat flux from 1 to 5 AU: Ulysses observations, *J. Geophys. Res., 99,* 23,401, 1994.

Solomon, J., N. Cornilleau-Wehrlin, P. Canu, D. Lengyel-Frey, S. J. Bame, E. E. Scime, A. Balogh, and R. Forsyth, Interaction between whistler-mode waves and electrons in the vicinity of interplanetary shocks as seen by Ulysses: A preliminary study, *Space Sci. Rev., 72,* 181, 1995.

Stix, T. H., *The Theory of Plasma Waves,* p.10, McGraw-Hill, New York, 1962.

Stone, R. G. et al., The Ulysses unified radio and plasma wave investigation, *Astron. Astrophys. Suppl. Ser., 92,* 291, 1992.

A. Balogh and R. Forsyth, The Blackett Laboratory, Imperial College of Science and Technology, London, England. email: r.forsyth@ic.ac.uk

R. A. Hess, NASA Goddard Space Flight Center, Code 690.2, Greenbelt, MD 20771. (email: roger.a.hess@gsfc.nasa.gov)

D. Lengyel-Frey, Johns Hopkins School of Medicine, Division of Oncology, Baltimore, MD 21287. (email: FREYDE@wpmail.onc.jhu.edu)

N. Lin, School of Physics and Astronomy, Univ. of Minnesota, 116 Church Street, S. E., Minneapolis, MN 55455. (email: lin@waves.space.umn.edu)

R. J. MacDowall, Laboratory for Extraterrestrial Physics, NASA Goddard Space Flight Center, Code 695, Greenbelt, MD 20771. (email: robert.j.macdowall@gsfc.nasa.gov)

R. G. Stone, Laboratory for Extraterrestrial Physics, NASA Goddard Space Flight Center, Code 690, Greenbelt,MD 20771. (email: robert.g.stone@gsfc.nasa.gov)

(Received September 21, 1995; revised January 19, 1996; accepted February 15, 1996.)